express
polymer letters

Research article

Factors and processes determining the impact resistance of PP impact copolymers with multi-phase structure

Milán Ferdinánd[1,2*] [ID]*, Michael Jerabek*[3] [ID]*, Róbert Várdai*[1,2] [ID]*, Emese Pregi*[1,2] [ID]*,*
Thomas Lummerstorfer[3]*, Markus Gahleitner*[3] [ID]*, Gábor Faludi*[1,2] [ID]*, János Móczó*[1,2] [ID]*,*
Béla Pukánszky[1,2] [ID]

[1]Laboratory of Plastics and Rubber Technology, Department of Physical Chemistry and Materials Science, Faculty of Chemical Technology and Biotechnology, Budapest University of Technology and Economics, Műegyetem rkp. 3., H-1111 Budapest, Hungary
[2]Institute of Materials and Environmental Chemistry, Research Centre for Natural Sciences, HUN-REN, Magyar Tudósok Körútja 2., H-1117 Budapest, Hungary
[3]Borealis Polyolefine GmbH, St.-Peter-Strasse 25, A-4021 Linz, Austria

Abstract. The impact resistance of four polypropylene impact copolymers (ICPs) with multi-phase structures and widely differing characteristics was related to their structure. Blends were prepared from one of them and a high-density polyethylene (HDPE) to improve impact strength further. The structure of the materials was characterized by microscopy and dynamic mechanical thermal analysis. Mechanical properties were determined by tensile and impact testing, while local deformation processes were followed by volume strain measurements. The results obtained in the study proved that the shear-yielding of the matrix contributes the most among local processes to the increase of impact strength, while cavitation has a small effect on this latter property since its energy absorption is negligible. Both increasing elastomer content and decreasing particle size favor shear-yielding, thus improving impact strength. Considering the importance of elastomer content and elastomer particle size, a simple but very good model was created describing the dependence of the impact strength of ICPs on these latter two factors by using linear regression analysis. Although the addition of HDPE increases the fracture resistance of ICPs further, the extent of improvement is moderate, and the approach is economically disadvantageous.

Keywords: injection molding, copolymers, elastomer, impact behaviour, local deformation processes, failure modeling

1. Introduction

Polypropylene (PP) is one of the most advantageous polymers for the production of a large variety of packaging materials, consumer goods, and structural parts [1, 2]. The main advantage of PP over other raw materials is its beneficial cost/performance ratio; extensively used homopolymer (hPP) grades are available at a reasonable price, and they have sufficiently large modulus, deformability, and acceptable tensile strength [3]. Besides its advantages, one of the major drawbacks of hPP is its poor impact resistance of

around 2 kJ/m^2 at the melt flow rate (MFR) typical for injection molding [4]. In order to overcome the problem and thus extend the application area of PP even further, the polymer is routinely modified. Although synthetic polymer fibers have been recently used as impact modifiers [5–9] and attempts have been made to use high-density polyethylene (HDPE) for the improvement of impact resistance [10–12], the traditional way to achieve this goal is the addition of elastomers [13–15]. Melt blending of hPP with amorphous ethylene-propylene copolymers (EPR)

or ethylene-propylene-diene terpolymers (EPDM) results in physical blends and is a well-developed technology known for decades [16–20]. However, copolymerization carried out directly in the reactor offers an economically more feasible way to produce impact-modified PP grades. Such a technology involves the production of hPP followed by the downstream gas phase copolymerization of ethylene and propylene at various ratios to form a dispersed ethylene-propylene copolymer phase (EPC) of varying crystallinity [21–23]. The products formed in the sequential polymerization process are called impact copolymers (ICPs) or heterophasic copolymers because of their specific morphology. The structure of these materials is rather complex, consisting of the PP matrix itself, the dispersed particles of the amorphous EPC, and, depending on the composition of the copolymer, a certain amount of crystalline PE located within the elastomer particles [24–29]. The structure of the copolymers is a very important factor since the size of the dispersed elastomer particles is claimed to have an optimum value for efficient impact modification [27, 30, 31]. Besides the proper selection of ethylene/propylene and molecular weight ratio during polymerization, as well as processing conditions, particle size can also be controlled by the addition of another component. Although its mechanism was not thoroughly explained in the open literature, HDPE has been used for the impact modification of ICPs [32–35]. The modifier is mostly found encapsulated by the elastomer and changes the size of this latter, thus influencing impact resistance [32, 34, 36, 37].

Under the effect of external load stress concentration develops around elastomer particles in ICPs because of the dissimilar elastic properties of the phases [38]. Heterogeneous stress distribution and local stress maxima initiate local deformation processes, which determine the deformation and failure mechanism and, thus, the macroscopic properties of these materials [27, 39, 40]. Although to a different extent, all local deformation processes absorb energy and thus influence impact strength [41]. Shear-yielding and cavitation are the main processes taking place in ICPs [27]. Shear-yielding, *i.e.*, the slipping of larger structural units of the matrix [42], was proven to consume energy the most efficiently among local processes [41]. Accordingly, this process is very important in the determination of impact strength. Cavitation of the elastomer results in the formation of voids

[39], but the effect of this latter process is rather controversial, and it may either decrease or increase impact resistance [43, 44].

Although PP impact copolymers have been widely used in engineering applications for a long time, a strong interest and need exist from both academia and industry for their further development. Despite the complexity of their morphology, the structure-property relationships of ICPs are more or less known. However, the research on these materials lacks quantitative correlations between their performance, mainly impact strength and the factors and processes determining it. The aim of the present study is to remedy the situation and analyze the dependence of the room temperature (23 °C) impact strength of ICPs on their elastomer content and elastomer particle size by using simple models created with the help of linear regression analysis. Since local deformation processes have a considerable effect on deformation and failure, and thus also on impact strength, they were also studied in detail both qualitatively and quantitatively. An attempt was made to increase the impact strength of the copolymers further by the addition of HDPE. The consequences of the results for practice are also discussed at the end of the paper.

2. Experimental
2.1. Materials

Four different ICPs produced by Ziegler Natta catalyst and triethylaluminium co-catalyst were selected for the study; all four grades were supplied by Borealis Polyolefine GmbH, Linz, Austria. In order to avoid the use of complicated trade names, the copolymers will be differentiated by their elastomer and ethylene content, assigning simplified names to them. Accordingly, the copolymers will be referred to as ICP14P, ICP15E, ICP25P, and ICP32E, respectively. The number in the names indicates the elastomer content in wt%, while the E or P denotes that the elastomer is rich in ethylene (E) or propylene (P). Elastomer content and ethylene content of the elastomer were determined at Borealis GmbH. Xylene cold soluble (XCS) fraction representing the elastomer content was measured at 25 °C according to the ISO 16152 standard using laboratory equipment. The approach slightly underestimates elastomer content since xylene dissolves only the amorphous part of EPC, while crystalline regions remain in the xylene insoluble part (XCI) corresponding to the amount

of the matrix. The ethylene content of the elastomer (XCS) was determined by Fourier-transform infrared spectroscopy (Perkin Elmer infrared spectrometer FT-IR system 2000, Perkin Elmer, Waltham, MA, USA). The spectra were recorded on compression-molded films in the wavenumber range of 4000 and 400 cm^{-1}. To determine the composition, the absorption spectra were compared with library spectra calibrated by ^{13}C nuclear magnetic resonance (NMR) spectrometry in solution. Further details on the determination method can be found in [45]. Intrinsic viscosities (IV) of both XCS and XCI fractions were measured in decalin at 135 °C according to the DIN EN ISO 1628-1 and -3 standards in order to check molecular weight effects. A Lauda PVS automated capillary viscometer with Ubbelohde capillaries (Lauda, Lauda-Königshofen, Germany) was used for this purpose. The ICP32E polymer was also modified by blending with an HDPE homopolymer having a bimodal molecular weight distribution. A PP homopolymer intended for high-speed injection molding of products with long flow paths was used as a reference in the study. This latter was not identical to the matrix of the copolymers. Both the HDPE and the hPP were the products of Borealis. The studied polymers, together with their most important characteristics, are summarized in Table 1.

2.2. Processing, sample preparation

Blending with HDPE was carried out using a Brabender DSK 42/7 (Brabender GmbH, Duisburg, Germany) twin-screw compounder at the set temperatures of 190–200–205–210 °C and screw speed of 45 rpm. The amount of HDPE varied from 0 to 100 wt% in the blends in steps of 5 wt%. The granules of the blends, the four copolymers, the reference polymer, and the neat HDPE were injection molded into standard, ISO 527 1A tensile bars using a Demag Intelect 50/330-100 (Sumitomo Demag, Schwaig,

Germany) machine with the temperature profile of 190–200–205–210 °C. The rate of injection molding was 50 mm/s, the cooling time 40 s, and the holding time 30 s. The mold temperature was kept at 40 °C during processing. Injection molded specimens were stored at 23 °C and 50 *RH*% for one week before further testing. Plates of 1 mm thickness were compression molded from the four copolymers at 200 °C and 100 kN load for 3 min using a Fontijne SRA 100 machine (Fontijne Presses, Delft, The Netherlands).

2.3. Characterization, measurements

Tensile testing was carried out at 23 °C according to the ISO 527-2 standard using an Instron 5566 type universal testing machine (Instron, Norwood, MA, USA). Stiffness was determined at 0.5 mm/min cross-head speed and 115 mm gauge length, while characteristics measured at larger deformations were obtained at 5 mm/min cross-head speed and the same gauge length. Notched Charpy impact resistance was determined according to the ISO 179-1/1eC standard at 23 °C and 2 mm notch depth using a Ceast Resil 5.5 instrument (CEAST S.p.A., Pianezza, Italy) equipped with a hammer of 1 J capacity. Fracture surfaces of Charpy specimens were studied by scanning electron microscopy (SEM) using a Jeol JSM 6380 LA apparatus (Jeol Ltd., Tokyo, Japan). *N*-hexane was used to etch the elastomer particles from the cryo-fractured surfaces, resulting in holes left behind. Particle size was determined using the recorded micrographs by image analysis. 300 particles were measured for each sample. Transmission electron micrographs (TEM) of the copolymers were recorded on 85 nm thick slices. Before recording the micrographs, the sample was immersed in the aqueous solution of ruthenium tetroxide to increase contrast and thus allow the differentiation between regions with larger and smaller crystallinity. TEM analysis was carried out using a Tecnai 12 microscope (Fei Company,

Table 1. The most important characteristics of the polymers investigated in the study.

Polymer	Elastomer content [wt%]	Ethylene content of the elastomer [wt%]	IV$_{XCS}$ [dL/g]	IV$_{XCI}$ [dL/g]	Viscosity ratio IV$_{XCS}$/IV$_{XCI}$	MFR[a] [g/10 min]
ICP14P	14	27	1.7	2.7	0.6	3.0
ICP15E	15	43	3.5	2.2	1.6	3.5
ICP25P	25	21	5.3	1.8	2.9	4.5
ICP32E	32	38	3.4	1.5	2.3	11.0
HDPE						0.7[b]
hPP						50.0

[a]determined at 230 °C, 2.16 kg
[b]determined at 190 °C, 2.16 kg

Eindhoven, The Netherlands) at the Institute for Electron Microscopy and Fine Structure Research (FELMI) in Graz, Austria. The images were taken with a CCD-Camera (Gatan Inc., Abingdon, UK). Volume strain (VOLS) measurements were performed by Borealis GmbH. The full-field strain on the front (x and y direction) was measured by using two cameras to establish digital image correlation (DIC). In general, DIC is based on the principle of following the change in the structure of a speckle pattern superimposed artificially on the surface of the specimen during deformation by using an optical camera system. For the calculation of volume strain, the mean displacement of the speckles was determined on a small area at the front of the specimens in the x and y directions corresponding to the change of their dimensions in these directions. Dimensional change upon loading in the z direction was obtained by assuming that the relative strain in this latter direction is identical to that measured in the y one. In possession of the dimensions of the deformed specimen and that of the initial one volume strain was calculated at each elongation value by a software. Further details on the DIC test method can be found in [46]. Dynamic mechanical thermal analysis (DMTA) was carried out using a Perkin Elmer Diamond DMTA instrument (PerkinElmer, Waltham, MA, USA) on compression molded specimens with 50×5×1 mm dimensions between –120 and 80 °C at 1 Hz frequency, 10 μm deformation, and 2 °C/min heating rate in tension mode.

3. Results and discussion

The results are presented in several sections. The phase structure of the copolymers is characterized first and then tensile properties having relevance for the impact strength and fracture resistance of the copolymers are discussed subsequently. The effect of modification with HDPE on structure and properties is presented in the next section, followed by the analysis of local deformation processes. The most important findings and correlations are shown in the final section of the paper.

3.1. Phase structure

The copolymers investigated have heterogeneous structures consisting of evenly dispersed elastomer particles within the PP matrix, as shown in Figure 1a and 1b. These SEM micrographs recorded on the cryo-fractured surface of the ICP14P and ICP15E

copolymers also reveal that particle size can be very different even at practically the same elastomer content. The ICP14P with propylene-rich EPC has a finer structure than the ICP15E with ethylene-rich EPC; dispersed elastomer particles are hardly visible in Figure 1a. The TEM micrograph recorded on the ICP15E copolymer (Figure 1c) proves that the elastomer particle itself might also be heterogeneous, with a crystalline PE phase being embedded in the amorphous EPC. According to previous studies [24, 27], PE crystallizes above 50 wt% ethylene content of the elastomer, and the amount of crystalline PE encapsulated increases with the increase of this latter quantity.

The results of DMTA measurements (see Figure 2) offer further proof for the heterogeneous phase structure of the copolymers. The first peak observed at low temperature on the $\tan\delta$ *vs.* temperature correlation can be assigned to the relaxation transition of the elastomer while the other at higher temperature to that of the amorphous phase of PP. The intensity of the transition is more or less proportional to the amount of the relaxing phase; increasing elastomer content increases the intensity of the first transition while decreases that of the second. The glass transition temperature of the elastomer (T_g) is also different for the four copolymers. An ethylene-rich elastomer phase with larger chain mobility and weaker adhesion to the PP matrix has smaller T_g compared to the one containing more propylene [25, 47].

The effect of composition on the characteristics of ICPs is demonstrated quantitatively by the characteristics of the relaxation transitions of the phases (Table 2). The results of particle size analysis are also included in the table. The ethylene content of the elastomer influences particle size, which is larger for copolymers containing an elastomer rich in ethylene. However, it is important to note that besides ethylene content, the size of the elastomer particles is also affected by the viscosity ratio of the phases, *i.e.*, the elastomer and the matrix, and processing conditions [37, 48]. Based on the data compiled in Table 1, it seems that a smaller viscosity ratio favors the formation of smaller particles. However, the effect of these latter factors, *i.e.* ethylene content of the elastomer and the viscosity ratio of the phases, on particle size cannot be separated unambiguously.

3.2. Properties

The results presented in the previous section have shown that the phase structure of the copolymers
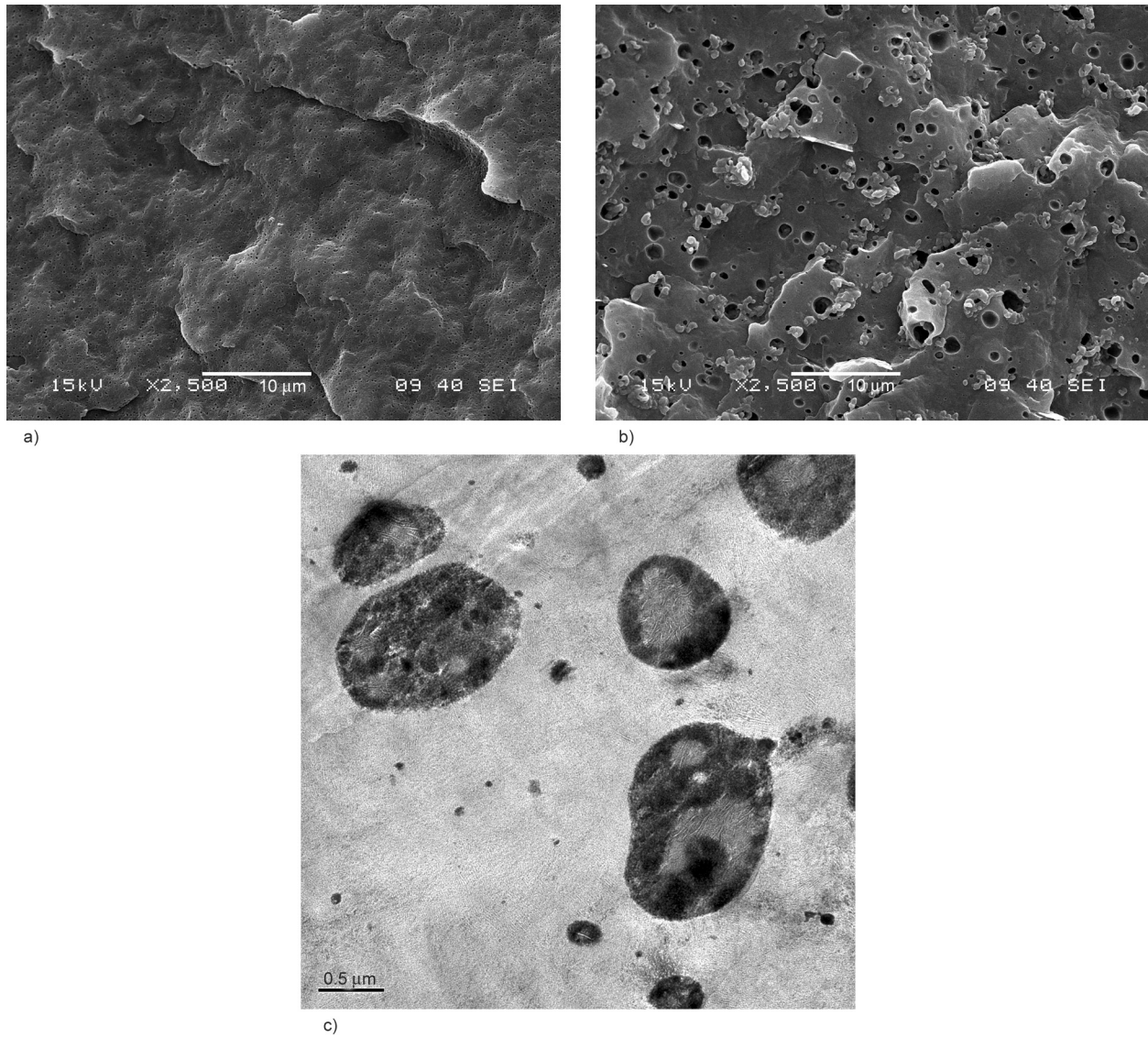
Figure 1. Phase structure of the ICPs studied. SEM micrographs recorded on cryo-fractured surfaces and TEM image. a) SEM, ICP14P, magnification: 2500×, b) SEM, ICP15E, magnification: 2500×, c) TEM, ICP15E, magnification: 26 000×.
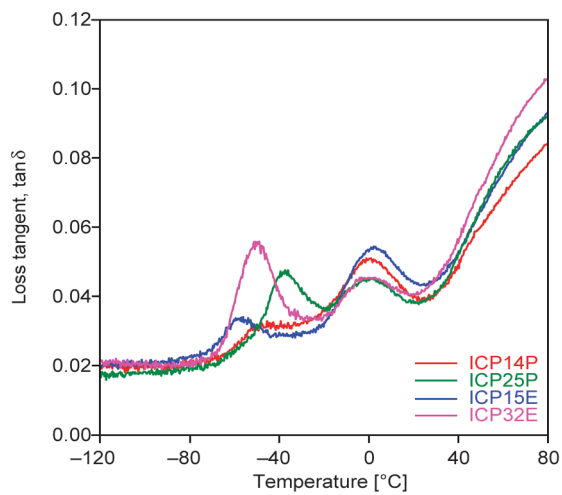

Figure 2. Relaxation transitions in ICPs. Loss tangent (tan δ) *vs.* temperature correlations determined by DMTA measurements.

Table 2. Characterization of the phase structure of the ICPs studied; DMTA measurements and particle size analysis.

Polymer	Relaxation transitions				Mean particle size of the elastomer [μm]
	Elastomer		Polypropylene		
	T_g [°C]	tan δ	T_g [°C]	tan δ	
ICP14P	−48.6	0.032	0.3	0.051	0.11±0.03
ICP15E	−58.2	0.034	2.8	0.054	0.72±0.35
ICP25P	−38.4	0.047	0.6	0.045	0.65±0.25
ICP32E	−50.7	0.056	−0.5	0.045	0.81±0.30

varies in a wide range. This fact might make the identification of the main factors determining their properties difficult. Young's modulus is important for impact modification since it is related to the resistance of the material against deformation. The
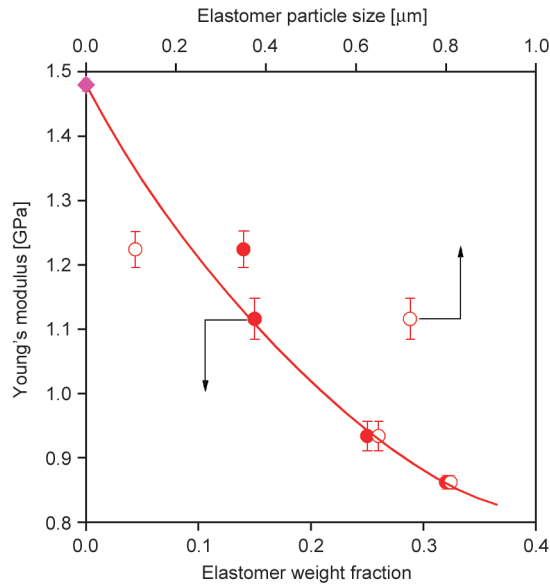
Figure 3. Young's modulus of ICPs plotted as a function of elastomer content and particle size. Full symbols: elastomer content, empty symbols: particle size, purple diamond: hPP reference.
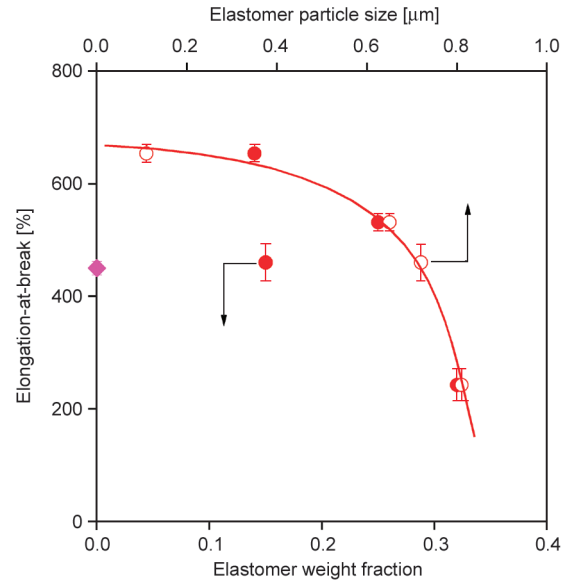

Figure 4. The dependence of the elongation-at-break of ICPs on elastomer content and particle size. Full symbols: elastomer content, empty symbols: particle size, purple diamond: hPP reference.

Young's modulus of the copolymers is plotted as a function of elastomer content and particle size in Figure 3. Although particle size influences modulus somewhat, elastomer content seems to dominate this property. This observation is not surprising, as the presence of soft inclusions always decreases stiffness, and the effect becomes more pronounced with increasing amount of the elastomer.

In addition, elongation-at-break reflecting the overall deformability of the material can be related to impact resistance. As shown in Figure 4, elongation-at-break correlates strongly with particle size, while elastomer content has a less clear effect on it. The decrease in the deformability of the copolymers with increasing elastomer particle size must be related to local deformation processes taking place around the particles upon loading. The results indicate that smaller particles might be more beneficial for impact modification. Our assumption is corroborated further by the fact that similarly to elongation-at-break, the integrated area under the stress *vs.* strain curve, *i.e.*, the toughness, increases with decreasing particle size as well.

The dependence of the notched Charpy impact resistance of the copolymers on elastomer content and elastomer particle size is plotted in Figure 5. Both factors influence impact resistance at 23 °C, but further analysis is needed to define the effect of the two variables more exactly. Quite surprisingly, the ethylene content of the elastomer has no direct influence
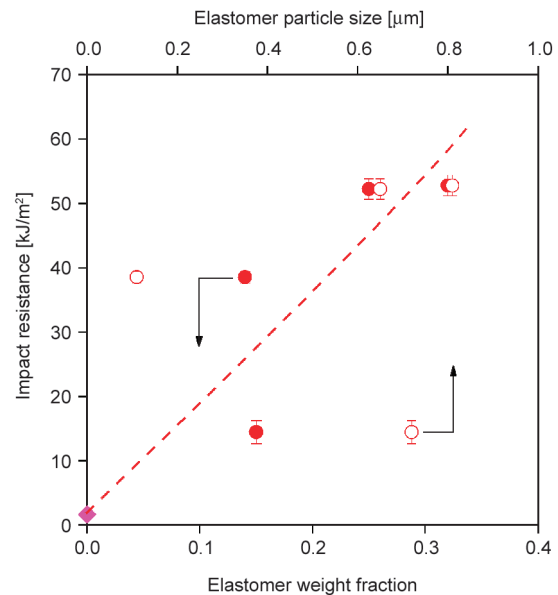

Figure 5. Notched Charpy impact resistance of ICPs. Effect of elastomer content and particle size. Full symbols: elastomer content, empty symbols: particle size, purple diamond: hPP reference.

on the properties of the copolymers because of its overlapping effect with other factors and the limited number of materials investigated.

3.3. HDPE modification

According to literature sources, embedded structure forms commonly upon the addition of HDPE to PP impact copolymers [33, 36, 37]. Indeed, as shown by the SEM micrographs recorded on the cryo-fractured
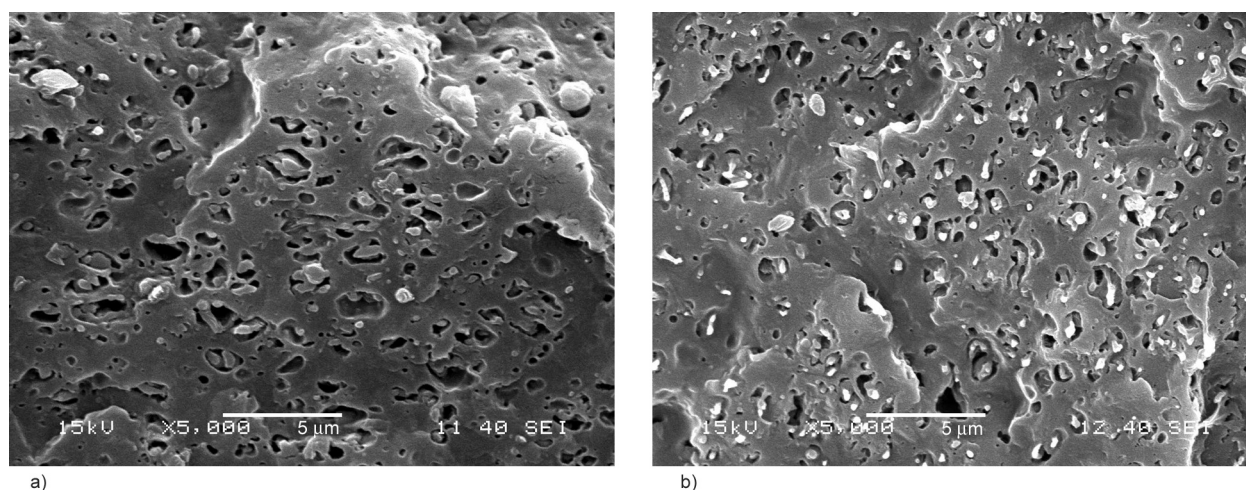
Figure 6. Embedded structure of ICP32E/HDPE blends. SEM micrographs taken on cryo-fractured surfaces. a) 10 wt% HDPE, b) 20 wt% HDPE. Magnification: 5000×.

surface (see Figure 6) of selected ICP32E/HDPE blends, the modifier is located mainly within the elastomer particles and forms a common phase with the already existing crystalline PE inclusions. The minimum observed at 25 wt% HDPE content on the modulus *vs.* composition correlation (not shown) offers further evidence for extensive embedding up to this composition. The images presented also indicate that by increasing the amount of HDPE, the dispersed structure of the blends becomes more homogeneous, and the size of the elastomer particles decreases. Particle size decreases continuously from 0.8 to 0.4 μm by increasing HDPE content from 0 to 25 wt% in the

Figure 7. Notched Charpy impact resistance of ICP32E/HDPE blends plotted as a function of HDPE content and elastomer particle size. Full symbols: HDPE content, empty symbols: particle size, red circles: neat ICP32E copolymer.

ICP32E copolymer. The effect of the amount of HDPE content on the notched Charpy impact resistance of the ICP32E copolymer is shown in Figure 7, together with the effect of particle size. HDPE improves impact strength from 53 to around 68 kJ/m^2 since it increases the effective elastomer content of the copolymer by embedding, on the one hand, and decreases the size of the particles, on the other. The observed changes in structure are favorable for impact modification, even if to a limited extent.

3.4. Local processes
SEM micrographs on fractured surfaces offer valuable information on local deformation processes occurring in the material under the effect of external load. Such micrographs are presented in Figure 8, taken on the ICP15E and ICP32E copolymers, respectively. The large voids observed in both images indicate that intensive cavitation takes place in the copolymers during fracture. The whitening of the surface around voids visible on the micrograph of the ICP32E copolymer (Figure 8b) proves that besides cavitation, the other main local process is the shear-yielding of the PP matrix in the copolymers.
The results of volume strain measurements shown in Figure 9a corroborate our observations made above even further. The large volume increase measured for all copolymers is the result of the cavitation of the elastomer particles since the shear-yielding of the matrix is not accompanied by volume increase. The extent of cavitation might depend on several factors, such as the elastomer content of PP, composition and the properties of the elastomer and its particle size as well. Copolymers containing ethylene-rich elastomer
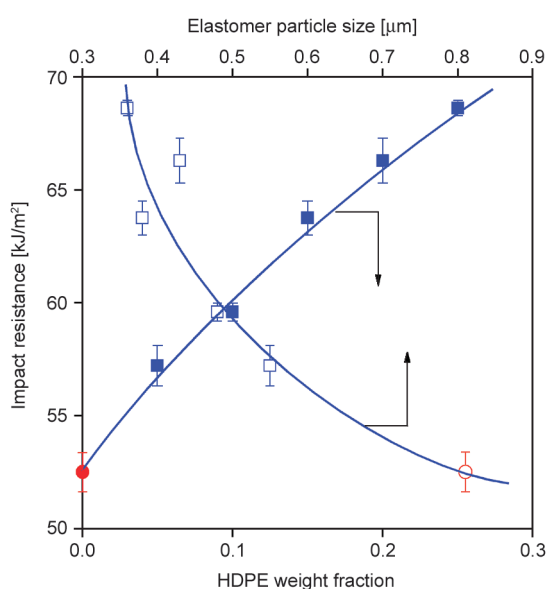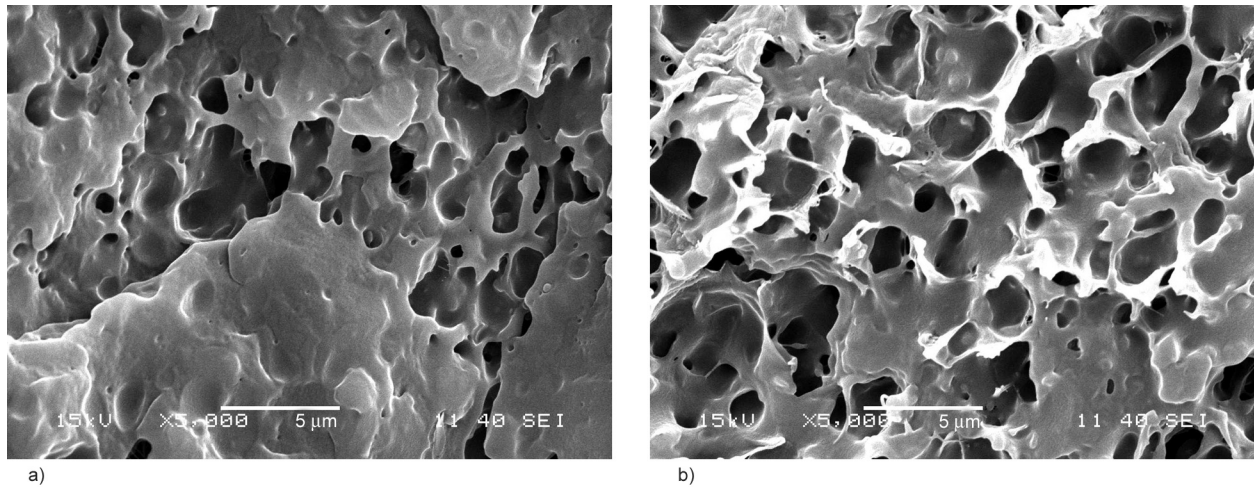
Figure 8. Local deformation processes taking place in ICPs. SEM micrographs, taken on elongated, fractured specimens. a) ICP15E, b) ICP32E. Magnification: 5000×.

seem to cavitate to a larger extent. Although not presented, very similar micrographs and volume strain traces were obtained for ICP blends containing HDPE, proving that the mechanism of the local deformation processes does not change upon HDPE modification.

The overall deformation of the copolymers can be divided into components with the help of the results of volume strain measurements; thus, local deformations can be analyzed further [49]. The analysis assumes the additivity of linear (Equation (1)) and volume strains (Equation (2)):

$$\varepsilon = \frac{\Delta l}{l_0} = \varepsilon_{el} + \varepsilon_{sh} + \varepsilon_{cav} \tag{1}$$

where ε is strain, Δl the change of length, l_0 the initial length of the specimen, while ε_{el}, ε_{sh}, ε_{cav} are the components of strain resulting from elastic deformation, shear-yielding, and cavitation. Similarly, also volume strain can be divided into components:

$$\frac{\Delta V}{V_0} = \left(\frac{\Delta V}{V_0}\right)_{el} + \left(\frac{\Delta V}{V_0}\right)_{cav} \tag{2}$$

where ΔV is volume change, and V_0 is the original volume of the specimen. It must be mentioned here that shear-yielding is not accompanied by volume increase; thus, total volume strain does not contain such a component.

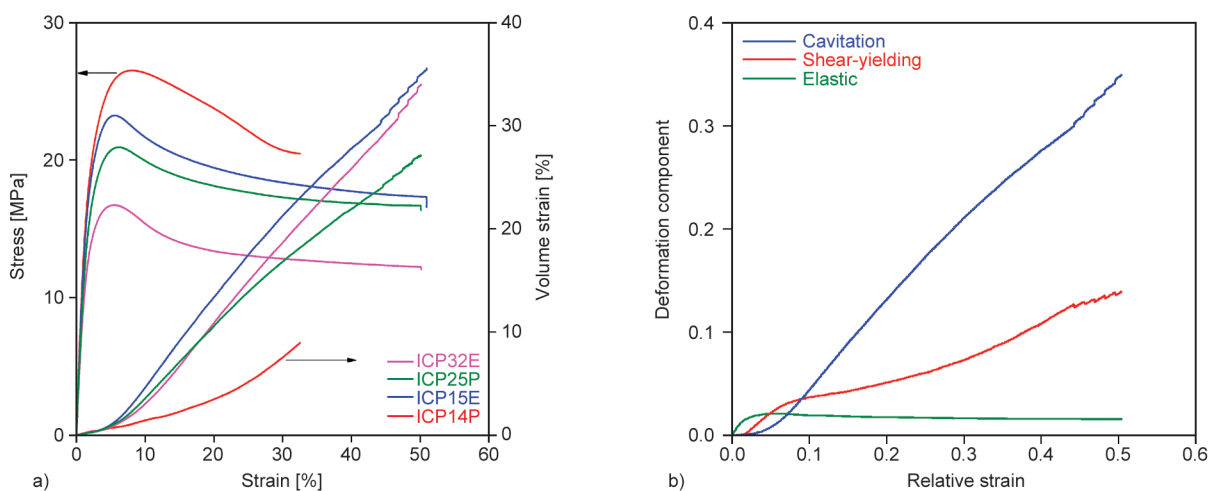From the definition of Poisson's ratio (Equation (3)) follows that:

Figure 9. Detection and analysis of local deformation processes occurring in ICPs. a) Results of volume strain measurements. The determination of volume was carried out by following the change in specimen dimensions continuously during deformation by using a camera system. Stress-strain correlations are plotted as reference. b) Deconvolution of overall deformation for the ICP15E copolymer.

$$\left(\frac{\Delta V}{V_0}\right)_{el} = (1 - 2\nu)\varepsilon_{el} \qquad (3)$$

where ν is the Poisson's ratio of the matrix, while as shown by Equation (4):

$$\varepsilon_{el} = \frac{\sigma}{E} \qquad (4)$$

where σ is stress and E is Young's modulus. Besides elastic deformation, only cavitation occurs in the matrix, but the elastic component assumes a positive value. Accordingly, the cavitation component of deformation in the matrix (Equation (5)) can be estimated as:

$$\varepsilon_{cav} = \left(\frac{\Delta V}{V_0}\right)_{cav} = \frac{\Delta V}{V_0} - \left(\frac{\Delta V}{V_0}\right)_{el} \qquad (5)$$

Finally, the shear-yielding component of deformation is obtained by subtracting all other components from the total deformation of the specimen (Equation (6)):

$$\varepsilon_{sh} = \varepsilon - \varepsilon_{el} - \varepsilon_{cav} \qquad (6)$$

The deconvolution of deformation was carried out for all materials investigated, and the result obtained for the ICP15E copolymer is presented in Figure 9b. As shown, the elastic component of deformation is very small and becomes practically constant after a certain elongation. On the other hand, the cavitation component is large and increases continuously with increasing strain. Although cavitation exceeds shear-yielding at larger strains, this latter is considerable as well and increases with elongation, similarly to cavitation.

3.5. Correlations

Stiffness and impact resistance are two key properties of impact-modified polymers. Therefore, these were plotted for all materials as a function of elastomer content, particle size, or both in Figures 10 and 11, respectively. Since HDPE is embedded in the elastomer and thus increases its amount, it is considered elastomer in further discussions. Stiffness is apparently dominated by and decreases considerably with increasing elastomer content (see Figure 10). Impact resistance is also influenced by elastomer content, but particle size also affects it; smaller particles seem to be more efficient in increasing impact strength than larger ones (see Figure 11). However, some points
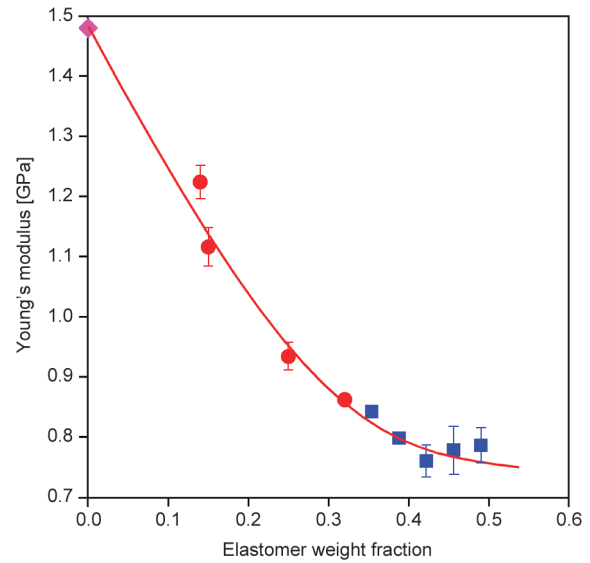

Figure 10. Young's modulus of impact-modified PP polymers plotted as a function of elastomer content. Symbols: (◆) hPP, (●) ICPs, (■) ICP32E/HDPE blends.
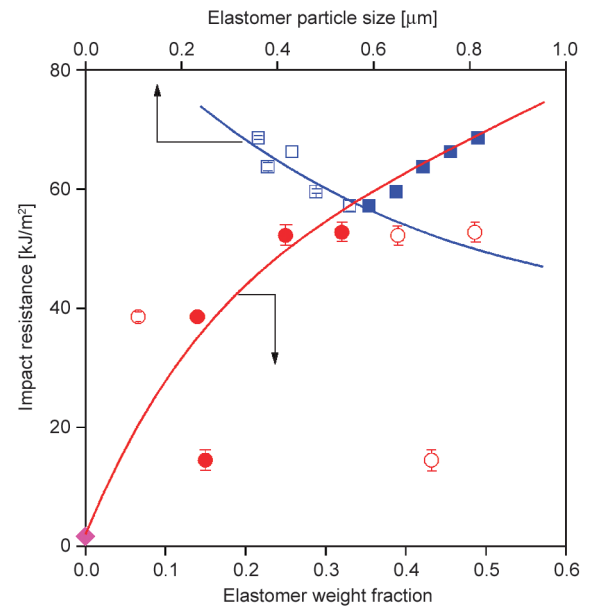

Figure 11. The dependence of the notched Charpy impact resistance of PP copolymers on elastomer content and elastomer particle size. Symbols: (◆) hPP, (○, ●) ICPs, (□, ■) ICP32E/HDPE blends; full symbols: elastomer content, empty symbols: particle size.

deviate significantly from both general trends indicating that the correlation is more complicated and thus impact resistance is also affected by further factors. The measured value of impact resistance is determined by the total energy absorbed by local deformation processes taking place upon loading. All processes consume energy, although to a different
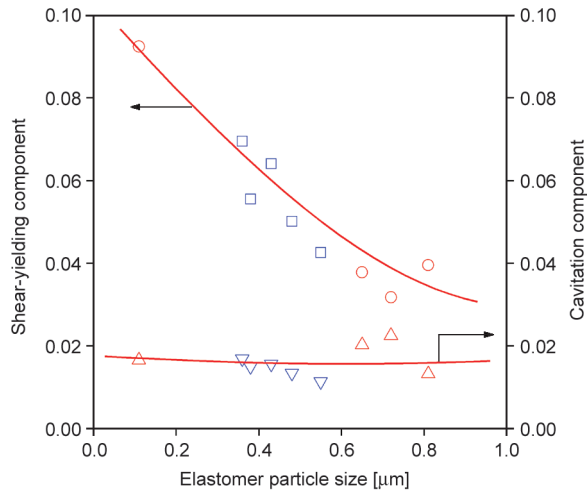
Figure 12. The shear-yielding and cavitation component of deformation plotted against the particle size of the elastomer. Symbols: (○) shear-yielding, ICPs, (□) shear-yielding, ICP32E/HDPE blends, (△) cavitation, ICPs, (▽) cavitation, ICP32E/HDPE blends.

extent. The shear-yielding and cavitation components of deformation were determined at the yield strain of the materials and they are plotted in Figure 12 as a function of particle size. As shown, shear-yielding decreases with increasing particle size, while cavitation remains practically constant in the entire particle size range. Quite similar observations were made for the effect of elastomer content since cavitation does not depend on this latter variable either. On the other hand, shear-yielding increases to some extent with increasing elastomer content (not shown).

Linear regression analysis was carried out using the Statistica software to find the correlation between impact resistance and some other properties of the materials studied. The model selected for demonstration (Equation (7)) includes Young's modulus and the shear-yielding component of deformation in the following way:

$$a_n = A + b_1 E + b_2 \varepsilon_{sh} \qquad (7)$$

where a_n is the notched Charpy impact resistance, A is interception, and b parameters are the coefficients for the effect of Young's modulus and shear-yielding on impact resistance. One might wonder about the selection of these two particular quantities for modeling. Modulus was taken into account since it reflects the resistance against deformation, as also shown by another model developed earlier [50], while the shear-yielding component of deformation

Table 3. Results of the modeling of the correlation between Young's modulus, the shear-yielding component of the deformation, and the impact resistance of ICPs (Equation (7)).

Property	Coefficient		Significance, p	R^2
	Parameter	Value		
Intercept	A	119.029	0.00005	
Young's modulus, E	b_1	−97.646	0.00024	0.8886
Shear-yielding, ε_{sh}	b_2	399.705	0.01009	

is proportional to the extent of the main energy-consuming local process [41]. The shear-yielding component of deformation used for the analysis was determined by the yield strain of the materials. The results of the model are collected in Table 3, together with the p values indicating the significance of the given variable at a 95% confidence level. The smaller the value of p, the larger the significance of the property. Significant components are printed in bold in the table. R^2 indicates the goodness of the fit. The nearly 0.9 value of this latter is quite large despite the simplicity of the model. According to the results, both the decrease in stiffness and the increase in the extent of shear-yielding taking place during deformation lead to improved impact resistance. Obviously, decreased stiffness decreases the resistance against shear-yielding, resulting in considerable energy consumption and, thus, increased impact resistance. The goodness of this simple correlation presented above is confirmed further by the results of Figure 13. As
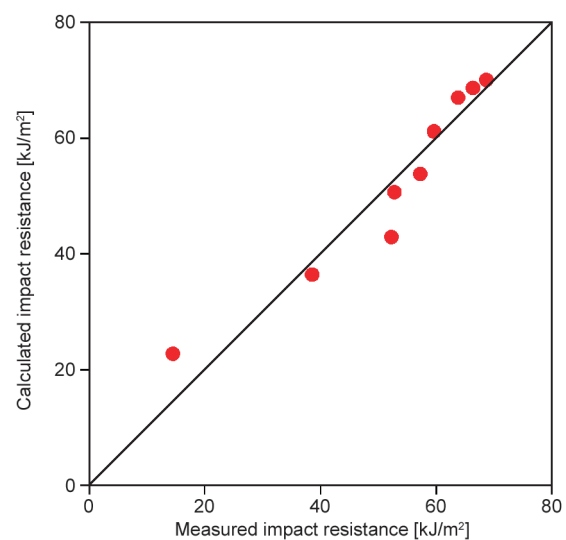

Figure 13. Correlation between the predicted (Equation (7)) and measured impact resistance of ICPs and their blends containing HDPE.

shown, the correlation between measured and predicted (Equation (7)) impact resistances is very close. Stiffness is determined by elastomer content, while particle size mainly defines shear-yielding, as shown earlier in this section. Accordingly, the modeling of impact resistance was carried out also by considering these two factors and their interaction as well (Equation (8)). The model created can be expressed as:

$$a_n = A + b_1 w_e + b_2 d_e + b_{12} d_e \qquad (8)$$

where the meaning of a_n, A, and b parameters are the same as in the previous model while w_e is the weight fraction of the elastomer and d_e is the particle size of this latter. The result of the analysis is summarized in Table 4, while the correlation between impact resistances measured and predicted by the model (Equation (8)) is plotted in Figure 14. The most important message of the model is that elastomer content is not

the sole factor influencing impact strength, particle size is equally important. However, the ethylene content of the elastomer is not represented in the analysis since it could not be calculated properly for the blends prepared by the addition of HDPE because of the dissimilar effect of this latter on structure and properties compared to amorphous PE sequences introduced into the elastomer during polymerization. Increasing elastomer content and decreasing particle size increase the amount of soft interphase formed at the contact surface of the PP matrix and the elastomer. The increasing amount of soft interphase leads to a larger extent of shear-yielding and, thus, to improved impact resistance. Finally, it should be noted here that the small p-value obtained for the interaction of elastomer content and particle size in the model indicates that these two factors are not completely independent of each other.

Besides the general overview of the structure-property correlations of PP impact copolymers, which was the focus of the majority of previous studies, simple models were created for the first time with the help of linear regression analysis describing the dependence of the impact strength of these materials on various factors. Even if the models need further verification because of the number of simplifications applied as well as the omittance of certain characteristics, such as the ethylene content of the elastomer, they may contribute to the further development of impact-modified PP materials in the future.

The findings of the study also highlight the practical relevance of shear-yielding in impact modification. Modifiers promoting the considerable shear-yielding of the matrix polymer increase impact resistance efficiently. The extent of shear-yielding strongly depends on interfacial interactions; weak adsorption of polymer chains on the surface of the modifier favors the occurrence of this latter process. Contrary to the results of some earlier reports [43, 51], cavitation taking place in elastomer-modified PP has no detrimental effect on impact strength. However, the energy consumption of cavitation is negligible, and thus, it does not improve impact resistance either. Finally, it must be noted that the modification of ICPs with another component, HDPE, in this case, is not beneficial. The property improvement achieved is not significant, on the one hand, and the modification requires an additional processing step, which is not economical, on the other.

Table 4. Investigation of the main factors determining the impact resistance of ICPs. Results of the linear regression analysis based on Equation (8).

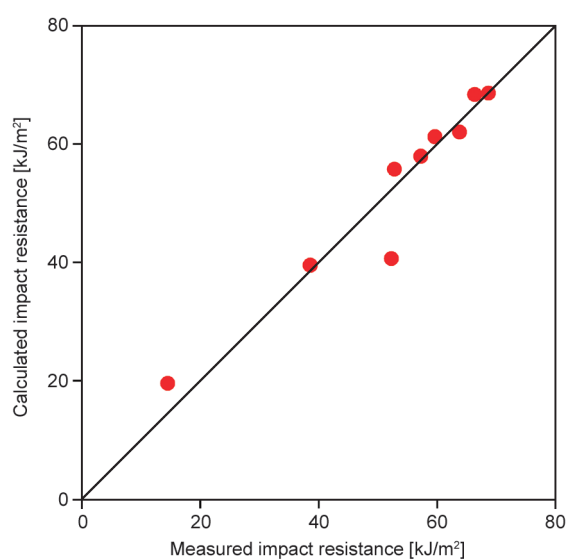| Factor	Coefficient		Significance, p	R^2
	Parameter	Value		
Intercept	A	41.832	0.01761	
Elastomer weight fraction, w_e	b_1	11.739	0.81174	
Elastomer particle size, d_e	b_2	−73.825	0.04161	0.8739
Weight fraction·particle size, $w_e d_e$	b_{12}	269.819	0.06039	

Figure 14. Impact resistance predicted by the model of Equation (8) plotted against measured values for ICPs and their blends with HDPE.

4. Conclusions

The results obtained on four different PP impact copolymers of multi-phase structure and on their blends with HDPE proved that elastomer content and elastomer particle size are equally important factors in determining impact resistance at ambient temperature (*i.e.*, above the T_g of the matrix hPP). Shear-yielding and cavitation are the main local deformation processes taking place in the copolymers upon loading. Large elastomer content and small particle size facilitate shear-yielding and thus improve impact strength. Contrary to shear-yielding, cavitation does not consume much energy; thus, its effect on impact resistance is small; it does not increase or deteriorate impact strength. The addition of HDPE to PP impact copolymers results in embedded structure and thus increases the effective elastomer content, on the one hand, and decreases particle size, on the other. Accordingly, HDPE improves impact resistance to some extent but not very efficiently.

Acknowledgements

References

[1] Maddah H. A.: Polypropylene as a promising plastic: A review. American Journal of Polymer Science, **6**, 1–11 (2016).
https://doi.org/10.5923/j.ajps.20160601.01

[2] Flowers B.: Automotive applications for polypropylene and polypropylene composites. in 'Handbook of polypropylene and polypropylene composites' (ed.: Karian H.) CRC Press, Boca Raton, 578–586 (2003).

[3] Tordjeman P., Robert C., Marin G., Gerard P.: The effect of α, β crystalline structure on the mechanical properties of polypropylene. The European Physical Journal E, **4**, 459–465 (2001).
https://doi.org/10.1007/s101890170101

[4] Gensler R., Plummer C. J. G., Grein C., Kausch H-H.: Influence of the loading rate on the fracture resistance of isotactic polypropylene and impact modified isotactic polypropylene. Polymer, **41**, 3809–3819 (2000).
https://doi.org/10.1016/S0032-3861(99)00593-5

[5] Várdai R., Ferdinánd M., Lummerstorfer T., Pretschuh C., Jerabek M., Gahleitner M., Faludi G., Móczó J., Pukánszky B.: Effect of various organic fibers on the stiffness, strength and impact resistance of polypropylene; A comparison. Polymer International, **70**, 145–153 (2020).
https://doi.org/10.1002/pi.6105

[6] Unterweger C., Brüggemann O., Fürst C.: Effects of different fibers on the properties of short-fiber-reinforced polypropylene composites. Composites Science and Technology, **103**, 49–55 (2014).
https://doi.org/10.1016/j.compscitech.2014.08.014

[7] Fu S., Yu B., Tang W., Fan M., Chen F., Fu Q.: Mechanical properties of polypropylene composites reinforced by hydrolyzed and microfibrillated kevlar fibers. Composites Science and Technology, **163**, 141–150 (2018).
https://doi.org/10.1016/j.compscitech.2018.03.020

[8] Maity J., Jacob C., Das C. K., Kharitonov A. P., Singh R. P., Alam S.: Fluorinated aramid fiber reinforced polypropylene composites and their characterization. Polymer Composites, **28**, 462–469 (2007).
https://doi.org/10.1002/pc.20303

[9] Asgari M., Masoomi M.: Thermal and impact study of PP/PET fibre composites compatibilized with glycidyl methacrylate and maleic anhydride. Composites Part B: Engineering, **43**, 1164–1170 (2012).
https://doi.org/10.1016/j.compositesb.2011.11.035

[10] Lin J-H., Pan Y-J., Liu C-F., Huang C-L., Hsieh C-T., Chen C-K., Lin Z-I., Lou C-W.: Preparation and compatibility evaluation of polypropylene/high density polyethylene polyblends. Materials, **8**, 8850–8859 (2015).
https://doi.org/10.3390/ma8125496

[11] Salih S., Hamood A. A., Alsalam A.: Comparison of the characteristics of LDPE: PP and HDPE: PP polymer blends. Modern Applied Science, **7**, 33–42 (2013).
https://doi.org/10.5539/mas.v7n3p33

[12] Tai C. M., Li R. K. Y., Ng C. N.: Impact behaviour of polypropylene/polyethylene blends. Polymer Testing, **19**, 143–154 (2000).
https://doi.org/10.1016/S0142-9418(98)00080-4

[13] Jafari S. H., Gupta A. K.: Impact strength and dynamic mechanical properties correlation in elastomer-modified polypropylene. Journal of Applied Polymer Science, **78**, 962–971 (2000).
https://doi.org/10.1002/1097-4628(20001031)78:5<962::AID-APP40>3.0.CO;2-5

[14] Galli P., Danesi S., Simonazzi T.: Polypropylene based polymer blends: Fields of application and new trends. Polymer Engineering and Science, **24**, 544–554 (1984).
https://doi.org/10.1002/pen.760240807

[15] Karger-Kocsis J., Kiss L.: Dynamic mechanical properties and morphology of polypropylene block copolymers and polypropylene/elastomer blends. Polymer Engineering and Science, **27**, 254–262 (1987).
https://doi.org/10.1002/pen.760270404

[16] Grestenberger G., Potter G. D., Grein C.: Polypropylene/ethylene-propylene rubber (PP/EPR) blends for the automotive industry: Basic correlations between EPR-design and shrinkage. Express Polymer Letters, **8**, 282–292 (2013).
https://doi.org/10.3144/expresspolymlett.2014.31

[17] D'Orazio L., Mancarella C., Martuscelli E., Polato F.: Polypropylene/ethylene-co-propylene blends: Influence of molecular structure and composition of EPR on melt rheology, morphology and impact properties of injection-moulded samples. Polymer, **32**, 1186–1194 (1991).
https://doi.org/10.1016/0032-3861(91)90220-D

[18] van der Wal A., Verheul A. J. J., Gaymans R. J.: Polypropylene–rubber blends: 4. The effect of the rubber particle size on the fracture behaviour at low and high test speed. Polymer, **40**, 6057–6065 (1999).
https://doi.org/10.1016/S0032-3861(99)00215-3

[19] Choudhary V., Varma H. S., Varma I. K.: Polyolefin blends: Effect of EPDM rubber on crystallization, morphology and mechanical properties of polypropylene/EPDM blends. 1. Polymer, **32**, 2534–2540 (1991).
https://doi.org/10.1016/0032-3861(91)90332-D

[20] Karger-Kocsis J., Kuleznev V. N.: Dynamic mechanical and impact properties of polypropylene/EPDM blends. Polymer, **23**, 699–705 (1982).
https://doi.org/10.1016/0032-3861(82)90054-4

[21] Gahleitner M., Tranninger C., Doshev P.: Heterophasic copolymers of polypropylene: Development, design principles, and future challenges. Journal of Applied Polymer Science, **130**, 3028–3037 (2013).
https://doi.org/10.1002/app.39626

[22] Encarnacion J. D., Park S. J., Ko Y. S.: Polymerization of heterophasic propylene copolymer with Me$_2$Si(2-Me-4-PhInd)$_2$ZrCl$_2$ supported on SiO$_2$ and SiO$_2$-MgCl$_2$ carriers. Korean Journal of Chemical Engineering, **37**, 380–386 (2020).
https://doi.org/10.1007/s11814-019-0450-4

[23] Galli P., Haylock J., Simonazzi T.: Manufacturing and properties of polypropylene copolymers. in 'Polypropylene structure, blends and composites' (eds.: Karger-Kocsis J.) Springer, Dordrecht, Vol. **2**, 1–24 (2003).
https://doi.org/10.1007/978-94-011-0521-7_1

[24] Radusch H-J., Doshev P., Lohse G.: Phase behavior and mechanical properties of heterophasic polypropylene-ethylene/propylene copolymers systems. Polimery, **50**, 279–285 (2005).

[25] Doshev P., Lohse G., Henning S., Krumova M., Heuvelsland A., Michler G., Radusch H-J.: Phase interactions and structure evolution of heterophasic ethylene–propylene copolymers as a function of system composition. Journal of Applied Polymer Science, **101**, 2825–2837 (2006).
https://doi.org/10.1002/app.22921

[26] Botha L., Sinha P., Joubert S., Duveskog H., van Reenen A. J.: Solution and solid-state NMR characterization of heterophasic propylene–ethylene copolymers (HEPC) with increasing ethylene content. European Polymer Journal, **59**, 94–104 (2014).
https://doi.org/10.1016/j.eurpolymj.2014.07.010

[27] Doshev P., Lach R., Lohse G., Heuvelsland A., Grellmann W., Radusch H. J.: Fracture characteristics and deformation behavior of heterophasic ethylene–propylene copolymers as a function of the dispersed phase composition. Polymer, **46**, 9411–9422 (2005).
https://doi.org/10.1016/j.polymer.2005.07.029

[28] Rungswang W., Saendee P., Thitisuk B., Pathaweeisariyakul T., Cheevasrirungruang W.: Role of crystalline ethylene-propylene copolymer on mechanical properties of impact polypropylene copolymer. Journal of Applied Polymer Science, **128**, 3131–3140 (2013).
https://doi.org/10.1002/app.38495

[29] Santonja-Blasco L., Rungswang W., Alamo R. G.: Influence of chain microstructure on liquid–liquid phase structure and crystallization of dual reactor Ziegler–Natta made impact propylene–ethylene copolymers. Industrial and Engineering Chemistry Research, **56**, 3270–3282 (2017).
https://doi.org/10.1021/acs.iecr.6b04708

[30] Karger-Kocsis J., Csikai I.: Skin-core morphology and failure of injection-molded specimens of impact-modified polypropylene blends. Polymer Engineering and Science, **27**, 241–253 (1987).
https://doi.org/10.1002/pen.760270403

[31] Speri W. M., Patrick G. R.: Fiber reinforced rubber modified polypropylene. Polymer Engineering and Science, **15**, 668–672 (1975).
https://doi.org/10.1002/pen.760150906

[32] Jang H. J., Kim S-D., Choi W., Chun Y. S.: Morphology and stress whitening of heterophasic poly(propylene) copolymer/high density polyethylene blends. Macromolecular Symposia, **312**, 34–42 (2012).
https://doi.org/10.1002/masy.201100021

[33] Petrović Z. S., Budinski-Simendić J., Divjaković V., Škrbić Ž.: Effect of addition of polyethylene on properties of polypropylene/ethylene–propylene rubber blends. Journal of Applied Polymer Science, **59**, 301–310 (1996).
https://doi.org/10.1002/(SICI)1097-4628(19960110)59:2<301::AID-APP15>3.0.CO;2-Z

[34] Vranjes N., Rek V.: Effect of EPDM on morphology, mechanical properties, crystallization behavior and viscoelastic properties of iPP+HDPE blends. Macromolecular Symposia, **258**, 90–100 (2007).
https://doi.org/10.1002/masy.200751210

[35] Liu X., Miao X., Guo M., Song W., Shao J.: Influence of the HDPE molecular weight and content on the morphology and properties of the impact polypropylene copolymer/HDPE blends. RSC Advances, **5**, 80297–80306 (2015).
https://doi.org/10.1039/C5RA08517A

[36] Zhu W., Zhang X., Feng Z., Huang B.: Effect of ethylene-propylene copolymer with residual PE crystallinity on mechanical properties and morphology of PP/HDPE blends. Journal of Applied Polymer Science, **58**, 551–557 (1995).
https://doi.org/10.1002/app.1995.070580309

[37] Gahleitner M., Hauer A., Bernreitner K., Ingolic E.: PP-based model compounds as tools for the development of high-impact-ethylene-propylene copolymers. International Polymer Processing, **17**, 318–324 (2002).
https://doi.org/10.3139/217.1709

[38] Goodier J. N.: Concentration of stress around spherical and cylindrical inclusions and flaws. Journal of Applied Mechanics, **55**, 39–44 (1933).
https://doi.org/10.1115/1.4012173

[39] Bucknall C. B., Karpodinis A., Zhang X. C.: A model for particle cavitation in rubber-toughened plastics. Journal of Materials Science, **29**, 3377–3383 (1994).
https://doi.org/10.1007/BF00352036

[40] Lazzeri A., Bucknall C. B.: Dilatational bands in rubber-toughened polymers. Journal of Materials Science, **28**, 6799–6808 (1993).
https://doi.org/10.1007/BF00356433

[41] Ferdinánd M., Jerabek M., Várdai R., Lummerstorfer T., Pretschuh C., Gahleitner M., Faludi G., Móczó J., Pukánszky B.: Impact modification of wood flour reinforced PP composites: Problems, analysis, solution. Composites Part A: Applied Science and Manufacturing, **167**, 107445 (2023).
https://doi.org/10.1016/j.compositesa.2023.107445

[42] Bucknall C.: Deformation mechanisms in glassy polymers. in 'Toughened plastics' (eds.: Bucknall C.) Applied Science Publisher, London, 136–181 (1977).
https://doi.org/10.1007/978-94-017-5349-4_6

[43] Sudár A., Renner K., Móczó J., Lummerstorfer T., Burgstaller C., Jerabek M., Gahleitner M., Doshev P., Pukánszky B.: Fracture resistance of hybrid PP/elastomer/wood composites. Composite Structures, **141**, 146–154 (2016).
https://doi.org/10.1016/j.compstruct.2016.01.031

[44] Pawlak A., Galeski A., Rozanski A.: Cavitation during deformation of semicrystalline polymers. Progress in Polymer Science, **39**, 921–958 (2014).
https://doi.org/10.1016/j.progpolymsci.2013.10.007

[45] Aarnio-Winterhof M., Doshev P., Seppälä J., Gahleitner M.: Structure-property relations of heterophasic ethylene-propylene copolymers based on a single-site catalyst. Express Polymer Letters, **11**, 152–161 (2017).
https://doi.org/10.3144/expresspolymlett.2017.16

[46] Jerabek M., Major Z., Lang R. W.: Strain determination of polymeric materials using digital image correlation. Polymer Testing, **29**, 407–416 (2010).
https://doi.org/10.1016/j.polymertesting.2010.01.005

[47] Grein C., Bernreitner K., Gahleitner M.: Potential and limits of dynamic mechanical analysis as a tool for fracture resistance evaluation of isotactic polypropylenes and their polyolefin blends. Journal of Applied Polymer Science, **93**, 1854–1867 (2004).
https://doi.org/10.1002/app.20606

[48] Fortelný I., Kamenická D., Kovář J.: Effect of the viscosity of components on the phase structure and impact strength of polypropylene/ethylene-propylene elastomer blends. Die Angewandte Makromolekulare Chemie, **164**, 125–141 (1988).
https://doi.org/10.1002/apmc.1988.051640110

[49] Heikens D., Sjoerdsma S. D., Coumans W. J.: A mathematical relation between volume strain, elongational strain and stress in homogeneous deformation. Journal of Materials Science, **16**, 429–432 (1981).
https://doi.org/10.1007/BF00738633

[50] Pukánszky B., Maurer F. H. J.: Composition dependence of the fracture toughness of heterogeneous polymer systems. Polymer, **36**, 1617–1625 (1995).
https://doi.org/10.1016/0032-3861(95)99007-H

[51] Keledi G., Sudár A., Burgstaller C., Renner K., Móczó J., Pukánszky B.: Tensile and impact properties of three-component PP/wood/elastomer composites. Express Polymer Letters, **6**, 224–236 (2012).
https://doi.org/10.3144/expresspolymlett.2012.25